J Comp Physiol A (1998) 182: 131–143

ORIGINAL PAPER

S. Amagai

Time coding in the midbrain of mormyrid electric fish. II. Stimulus selectivity in the nucleus exterolateralis pars posterior

Accepted: 25 June 1997

Abstract The anterior and posterior exterolateral nuclei (ELa and ELp) of the mormyrid midbrain are thought to play a critical role in the temporal analysis of the electric discharge waveforms of other individuals. The peripheral electroreceptors receiving electric organ discharges (EODs) of other fish project through the brainstem to ELa via a rapid conducting pathway. EODs, composed of brief, but stereotyped waveforms are encoded as a temporal pattern of spikes. From previous work, we know that phase locking is precise in ELa. Here it is shown that evoked potentials recorded from ELp show a similar high degree of phase locking, although the evoked potentials last much longer. Single-unit recordings in ELp reveal two distinct populations of neurons in ELp: type I cells are responsive to voltage step functions, and not tuned for stimulus duration; type II cells are tuned to a specific range of stimulus durations. Type II cells are less responsive than type I cells, tend to respond with bursts of action potentials rather than with single spikes, have a longer latency, show weaker time locking to stimuli, and are more sensitive to stimulus polarity and amplitude. The stimulus selectivity of type II cells may arise from convergence of type I cell inputs. Despite the loss of rapid conduction between ELa and ELp, analysis of temporal features of waveforms evidently continues in ELp, perhaps through a system of labeled lines.

Key words Electroreception · Electric communication · Weakly electric fish · Mormyrid electric fish · Knollenorgan

Abbreviations *ELa* nucleus exterolateralis pars anterior · *ELp* nucleus exterolateralis pars posterior · *EOCD* electric organ corollary discharge · *EOD* electric organ discharge · *EPSP* excitatory postsynaptic potential · *NELL* nucleus of the electrosensory lateral line lobe · *PTX* picrotoxin

Introduction

Among the weakly electric fish, the shape of the waveform of the electric organ discharges (EODs) is an important parameter in electrical communication (Hopkins and Bass 1981; Graff and Kramer 1992; McGregor and Westby 1992). At least in some species, discrimination is dependent on temporal and not spectral features of the individual EOD waveforms (Hopkins and Bass 1981; Hopkins and Westby 1986). In the African mormyrids, this time-domain analysis is thought to be performed by the Knollenorgan pathway (Moller and Szabo 1981; Hopkins 1986). The information about the EOD waveforms is first encoded by the Knollenorgan electroreceptors located all over the body surface. A receptor fires a single time-locked action potential only when the local region around it experiences a rapid voltage change that causes the outside of the body to become positive with respect to the inside (Hopkins and Bass 1981). For example, if a positive square-pulse current is applied from left to right, the receptors located on the left half of the body will fire at the onset of the stimulus and those on the right side fire at the termination of the stimulus. If a natural EOD is applied, the timing of the firings will depend on the positions and the polarities of rapid voltage transitions within the waveform (Hopkins and

S. Amagai
Section of Neurobiology and Behavior,
Seeley G. Mudd Hall, Cornell University,
Ithaca, NY 14853-2702, USA

Present address:
Department of Psychology, University of Maryland,
College Park, MD 20742, USA
Tel.: +1-301 405-6935; Fax: +1-301 314-9566;
e-mail: samagai@bss3.umd.edu

Offprint requests to:
C.D. Hopkins
Section of Neurobiology and Behavior,
Seely G. Mudd Hall,
Cornell University, Ithaca, NY 14853–2792, USA

Bass 1981; Hopkins 1986). The relative timing of receptor responses from different parts of the body is thought to encode the EOD waveform shape (Hopkins 1986).

The Knollenorgan pathway is characterized by a rapid conduction system from the periphery (Knollenorgan electroreceptors) via the primary afferents to the hindbrain nucleus of the electrosensory lateral line lobe (NELL) and up to the midbrain nucleus exterolateralis pars anterior (ELa) of the torus semicircularis (Enger et al. 1976; Szabo et al. 1979, 1983; Haugedé-Carré 1980; Bell et al. 1981). The analysis of temporal information is thought to take place in ELa (Szabo et al. 1979; Bell 1986). ELa consists of input axons from both left and right NELL carrying inputs from both sides of the body, large intrinsic GABAergic cells which terminate on other cells within ELa, and small cells that may process temporal information by comparing direct NELL input with indirect time-delayed input via large cells (Mugnaini and Maler 1987; Amagai et al. 1998).

In the companion paper (Amagai et al. 1998) we found units with precise phase locking to an outside-positive single voltage step in ELa, much like the Knollenorgans in the periphery. We did not find units with any dependence on the temporal features of presented stimuli. Our analysis of ELa did not include recordings from the small cells, because of their small size (3–7.5 μm) and adendritic morphology. However, the small cells send their output to nucleus exterolateralis pars posterior (ELp) (Haugedé-Carré 1979), so analysis of cells in ELp may yield insights into the processing of temporal information in this system. Field potential recording of ELp by Szabo et al. (1979) shows a short-latency (3 ms) sharp potential from ELa and a long-latency (8 ms) slow potential in response to external stimulation. The field potentials suggest that responses in ELa are tightly phase locked, but in ELp are not. This disparity between ELa and ELp neurons in response latency and in the degree of phase locking has led others to suggest that ELa is the critical site in the analysis of temporal information (Bell and Szabo 1986; Hopkins 1986). This idea is based upon the reasoning that an accurate analysis of EOD waveforms of submillisecond duration requires a rapidly conducting system with faithfully preserved temporal information. Once this critical analysis is carried out, the system can become less stringent in the preservation of temporal information. The activity in ELp might then reflect the nature of this temporal analysis, perhaps by showing selectivity to different temporal patterns of spike activity arising from the shape or the duration of the stimuli. An optimistic expectation based on this is that ELp is organized spatially according to temporal characteristics of the stimulus.

In this paper, I used extracellular-evoked field potentials, extracellular single-unit recordings and intracellular recordings to explore the physiology of ELp.

Materials and methods

Animal care, surgery, experimental tank, stimulation and intracellular recordings

The details for these procedures and the histological procedures for those experiments involving intracellular recordings were described in Amagai et al. (1998). As in that paper, the spinal electromotorneuron command volley that leads to an EOD in an uncurarized animal and persists under curare was recorded non-invasively, using wires placed near the tail to monitor the general condition of the animal. This command signal was also used in the extracellular field potential study to determine if the observed responses were derived from the Knollenorgan inputs.

Extracellular field potential

For differential recording of field potentials from ELa and ELp, I used broken-tipped borosilicate glass microelectrodes (o.d. = 1.0 mm, i.d. = 0.5 mm, tip diameter: 10 μm) filled with 3 $mol \cdot l^{-1}$ NaCl connected to a Grass P-15 amplifier and monitored on a oscilloscope (Tektronix 5000 series). The reference electrode was placed just above the ELp, but still immersed in the cerebrospinal fluid. To improve the signal to noise ratio of field potentials, responses were digitized at 40 kHz and averaged on a PDP-11/24 or 11/34 computer.

Extracellular single unit recordings

Extracellular single unit recordings used a similar set-up. The electrodes were pulled on a Sutter P-87 electrode puller at settings suitable for intracellular recording and the tip carefully broken or pulled at settings for patch-clamp electrodes using capillary glass (7740 glass, i.d. = 0.058 in; Richland Glass) which were then filled with Woods metal and electroplated with gold and platinum (modified from Dowben and Rose 1953). Best isolation was obtained using electrodes with tip diameter in the range of 6–10 μm which gave stable recordings over a period of several hours. Standard stimulus was a square pulse delivered 4 per second in left/right geometry. While searching for cells, the stimulus duration (0.01–50 ms), amplitude (over 30 dB in 1-dB steps, re: 270 mV cm^{-1}) and polarity (left positive/right positive) were varied while the electrode was advanced. After a cell was isolated, the cell was characterized by stimulating 200 times with the stimulus duration, amplitude and geometry that generated the best response. This was then repeated with different stimulus durations (or amplitude or geometry) to characterize the cell's duration dependence (or amplitude or geometry). Instead of digitizing and averaging as above, the cell output was passed through a window discriminator (Model 121, WPI) and stored as post stimulus raster data. The response probability was calculated by dividing the number of times the response occurred by the number of stimulus presentations. Mean spike number per response was calculated by dividing the number of spikes by the number of times the cell responded to stimuli.

Pharmacological procedures

To block GABA-mediated inhibition, a polyethylene tube (i.d. = 1.14 mm) was placed inside the cranial cavity and 200 $\mu mol \cdot l^{-1}$ picrotoxin (PTX) dissolved in Hickmann's saline was gravity fed. For washout, saline was substituted for PTX. In the course of flushing out the PTX, the saline solution filling the cranial cavity overflowed into the tank which eventually increased the conductivity of the tank water over a period of hours (starting at 200 $\mu S \cdot cm^{-1}$, increasing up to about 500 $\mu S \cdot cm^{-1}$).

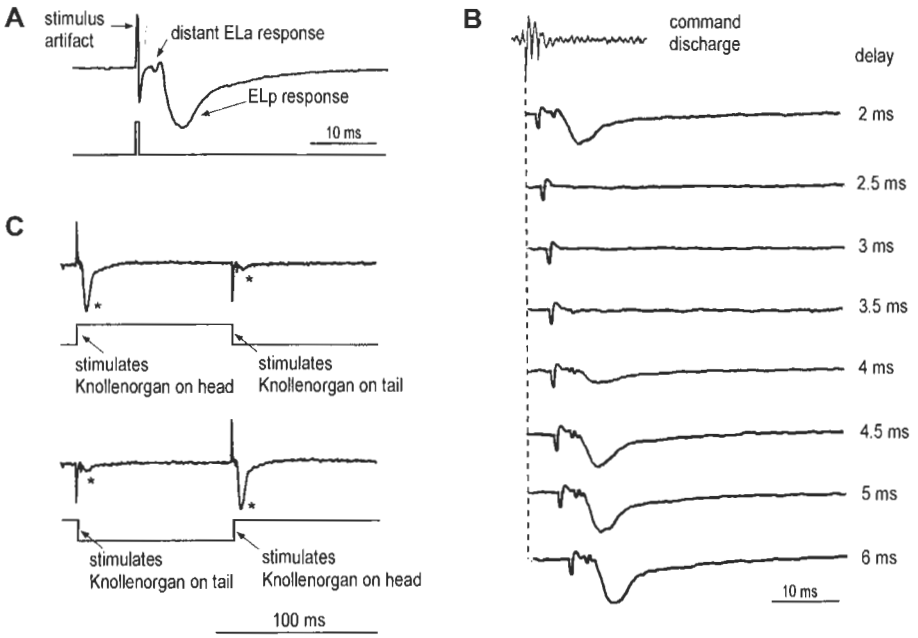

Fig. 1A–C Evoked potential of ELp. **A** *Top*: response to short duration (0.5 ms) pulsatile stimuli. *Bottom*: stimulus trace. Following the stimulus artifact are a small ELa response at a latency of 3 ms by volume conduction, and then a larger slower ELp response. **B** Inhibition of the evoked potentials owing to EOCD-derived inhibition. The sweeps were triggered by the electromotorneuron volley and stimuli of 0.5 ms duration were delivered at specific delays. If the delay was between 2.5 ms and 3.5 ms, both ELa and ELp responses were severely attenuated. Each trace in both (**A**) and (**B**) is an average of 20 responses. **C** ELp evoked potentials in response to long duration (100 ms) stimuli. *Top*: average of ten evoked potentials in ELp. *Bottom*: stimulus. Both the beginning and the end of the stimulus result in responses (*stars*) in ELp but the response to the stimulation of the head region is larger. There is no change in the amplitude of the evoked potentials for the head and the tail region if the stimulus presentation order was reversed (i.e., the polarity of the stimulus was reversed)

Results

Evoked potentials

An extracellular field potential recorded near the surface of ELp in response to a short rectangular pulse stimulus showed a sharp, short latency (3 ms), negative deflection (Fig. 1A). This event was synchronous with the large evoked potential in ELa and probably represented the activity of ELa recorded via passive spread of current into ELp (Szabo et al. 1979). The recording also showed a later (7 ms) broader negative wave that was characteristic of ELp (Fig. 1A). The wave lasted for approximately 10 ms and probably represented bursts of spikes from cells in ELp or prolonged synaptic activity. Both the early ELa response, and the later 10-ms response could be abolished by delivering the stimulus with a time delay of 2.5–3.5 ms with respect to the spinal electromotorneuron volley recorded near the tail (Fig. 1B). Inputs from the Knollenorgan pathway are blocked within NELL by strong inhibition by the electric organ corollary discharge (EOCD) that occurs at this time and normally serves to prevent reafference from the fish's own EOD (Bennett and Steinbach 1969; Russell and Bell 1978; Bell et al. 1981). Because the field potentials recorded were abolished at these delays, I conclude that they arise from the Knollenorgans and not from another electroreceptor type such as the fast-conducting mormyromasts.

When the fish was stimulated with a long-duration square-pulse stimulus, a single outside-positive voltage step was sufficient to elicit the field potential attributed to ELp (asterisks, Fig. 1C). The beginning and the end of the stimulus both elicited responses, representing inputs from stimulation of different regions of the body. The order in which different parts of the body were stimulated did not affect the magnitude of the response (Fig. 1C). Unlike ELa, the response of ELp varied in magnitude as a function of stimulus geometry. For head/tail and transverse stimulus configurations, both the onset and the end of the stimuli gave rise to evoked responses in ELp. The largest deflections occurred in response to stimulation of the head region (Fig. 2A, onset) and of the contralateral body surface (Fig. 2B, onset).

The evoked potentials from different surface regions of ELp showed variations in the peak amplitude of the response (Fig. 2). For the head/tail geometry stimulation, the largest responses were medial near the border of ELa and ELp and also in the area extending from the center of ELp to the lateral margin. At these locations, the ratio of the amplitude of the "head" response to that of the "tail" response was in the range of 4:1 to 6:1. In the regions that showed reduced amplitude of the head responses, the ratio of the head- to tail-evoked potentials were as low as 1.5:1 to 1:1. For the transverse geometry stimulation, the largest responses were obtained in the locations found most responsive in the head/tail geometry. The ratios of amplitudes to contralaterally stimulated to ipsilaterally stimulated responses were at most

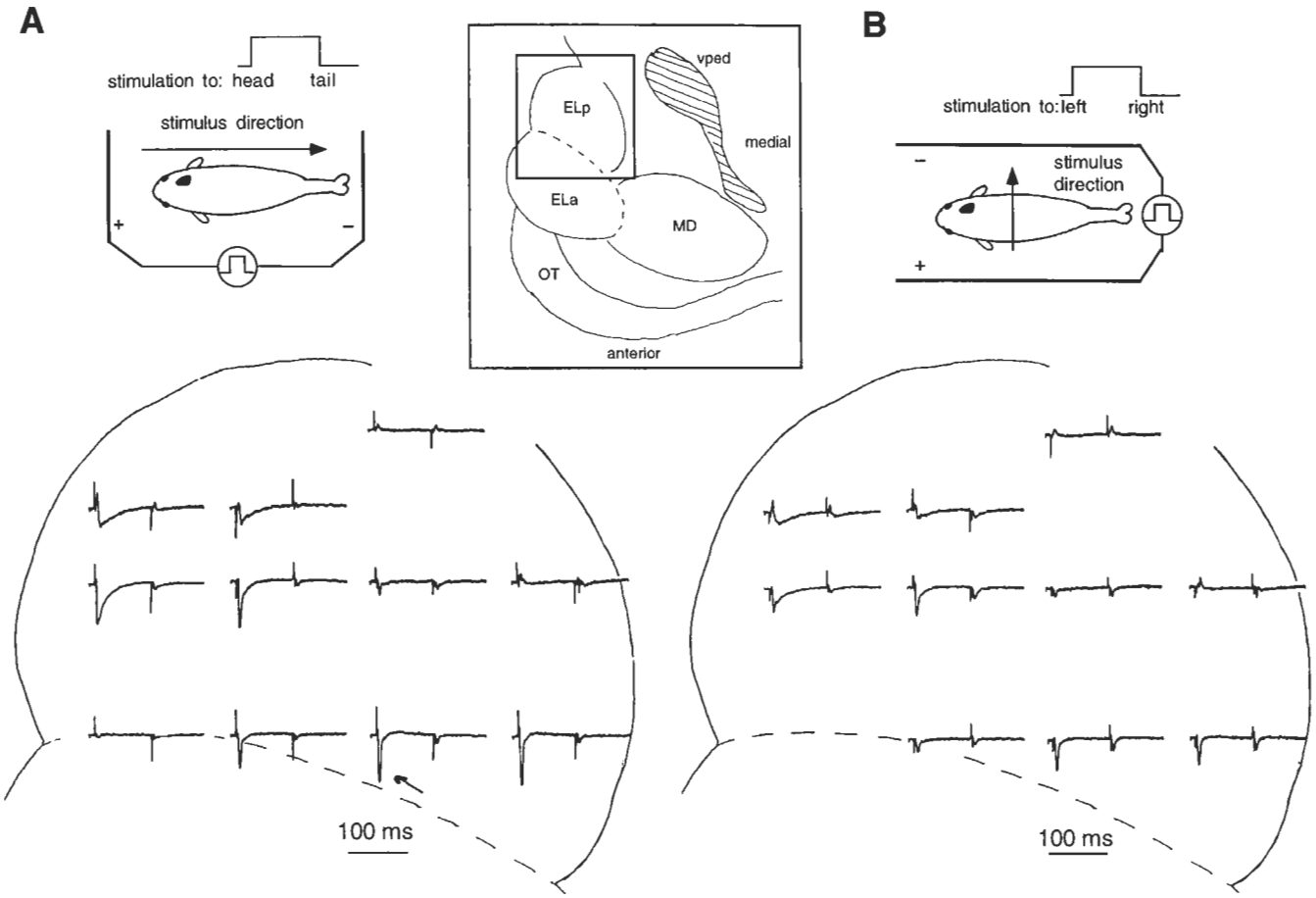

Fig. 2A, B Regional differences in the ELp evoked potentials. **A** Head/tail stimulation. Schematic diagram of the fish shows the stimulus direction. When the 100-ms stimulus comes on, the head region is stimulated, and when it goes off, the tail region is stimulated. *Inset*: a diagrammatic representation of ELp in dorsal view. Valvula cerebelli has been removed in this view (in the experiment, it was gently pushed out of the way), showing the cerebellar peduncle as a cross-hatched structure (*vped*). The region bounded by the *rectangle* is the area shown in expanded view on the bottom. Each evoked potential trace (average of ten sweeps) is centered in the recording location. **B** Transverse stimulation. Similar to **A** except for the stimulus geometry. *OT*: optic tectum, *MD*: nucleus medialis dorsalis

2:1 to 3:1 at the centrolateral border of ELa/ELp, dropping to about 1:1 in other regions.

The results from evoked potentials suggest the information carried into ELp lacks stimulus selectivity and has more in common with the selectivity at the periphery than hitherto assumed. Field potentials were evoked by simple voltage steps, and did not show obvious qualitative differences between different regions of ELp.

Extracellular single cell recordings

Extracellular recordings were made from single units in ELp to characterize the source of the evoked potential. Twenty-nine cells were isolated reliably enough for analysis. The cells could be inhibited by the EOCD (Fig. 3A), confirming that they were indeed being driven by inputs from the Knollenorgan system.

Unlike the Knollenorgan electroreceptors or cells in ELa, ELp neurons responded with a pattern of action potentials varying in both the latency and the number of spikes (Fig. 3B) in response to identical stimuli. ELp neurons also varied in their firing probability and their tendency to give bursting responses. For example, the cell on the left in Fig. 3C had a high firing probability. While this cell occasionally gave burst responses, most responses were single spikes or doublets. In the cell on the right in Fig. 3C, the firing probability was low (5/200) but the responses were exclusively bursts of up to seven spikes.

The population of cells encountered could be divided into two general cell types according to one criterion: those that responded like the evoked field potentials to a single outside-positive voltage step (type I cells), and those that required more complex stimulus characteristics (type II cells).

Type I cell characteristics

Type I cells responded to a square pulse stimulus by firing action potentials at a latency of 6–10 ms, as long as the stimulus duration was above a certain value. Their responsiveness varied little even to long stimuli with durations exceeding 10 ms. The minimum effective

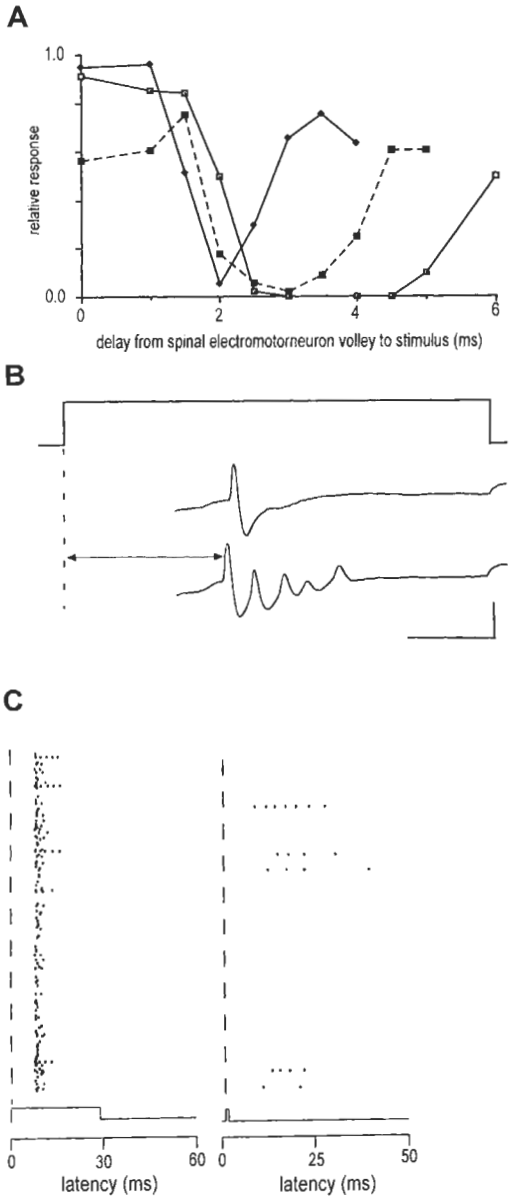

Fig. 3A–C Single unit recordings in ELp. **A** Inhibition of individual ELp responses by EOCD-derived inhibition. First, a stimulus parameter was found that elicited maximum response for a cell. Identical stimuli were then presented to the cell at a variable delay from the electromotorneuron volley. The resulting responses for three cells are plotted as the probability of response measure. The onset of inhibition was roughly similar in all three cells, while the end of the inhibition period was more variable. **B** Responses of a single ELp cell. This ELp neuron responded with action potentials of different numbers and latencies (*indicated by arrow*) in response to repetitive stimulations of a long stimulus. Two example responses are shown. The extracellular cell recordings were filtered at low pass: 100 Hz, high pass: 10 kHz. Scale bar at 150 μV and 5 ms. The stimulus was 25 ms long, 3 mV cm^{-1} in amplitude in transverse geometry. **C** Raster plots of two ELp cells showing different pattern of activity in response to 200 stimulations at 4 s^{-1}. *Left*: a type I cell that responded often to stimulation fired mostly single action potentials, but occasionally firing bursts of up to five action potentials. *Right*: a type II cell that responded rarely to stimulations fired only in bursts. The lines on the left of the raster plots define the zero time

stimulus duration varied greatly from cell to cell, ranging from 40 μs to >100 μs (Fig. 4A).

Type II cell characteristics

Type II cells were 'tuned' to stimulus duration, that is, they responded only to a restricted range of stimulus duration. The best duration (the one with the highest response probability) varied from <100 μs to >1 ms (Fig. 4B) for different type II cells. A stimulus outside this range elicited no response. Type II cells had latencies exceeding 10 ms.

Comparison of type I and type II cells

The categorization criterion of type I and type II cells correlated with additional response characteristics, summarized in Table 1 and discussed below. Apart from the difference in response latency, the two cell types showed overlap in all of these properties; these should therefore be treated as generalized tendencies of the behavior of the two cell types, rather than basis for categorization into type I or type II.

(1) Response probability. Type II cells responded rarely to repeated stimulations (e.g., Fig. 3C right). They were significantly less responsive than type I cells (Fig. 5A, Mann-Whitney U-test, $U_{9,9} = 70$, $P < 0.01$). The maximum responsiveness for type I cells approached 1:1 with the stimulus when the stimulus characteristics are optimal for that cell (e.g., Fig. 3C left; Fig. 5A). Only one type II cell had firing probability above 50%.

(2) Tendency to fire in bursts. The tendency for an ELp cell to fire in bursts of action potentials was unrelated to the response probability (Fig. 5A, $r = -0.263$, $df = 16$, NS). The distributions of mean spike number per response show that even though there were more examples of type II cells that responded with a large number of spikes, there was no statistical difference between the two groups in the number of action potential they fire per response (Fig. 5A, t-test, $n = 9$ in each group, $P > 0.05$).

(3) Latency and degree of time locking. Post stimulus time histograms showed that type I cells had latencies of 6–10 ms with a comparatively high degree of time locking (Fig. 5B). In contrast, type II cells showed latencies well in excess of 10 ms and had a highly variable response latency (Fig. 5B).

(4) Amplitude sensitivity. Type II cells showed a preference for a range of stimulus intensities, being inhibited at higher intensities. Type I cells do not show suppression of response at high intensities (Fig. 5D), even though there were exceptional cases (not shown).

(5) Polarity sensitivity. The two cell types were also differentially sensitive to the polarity of the stimulus:

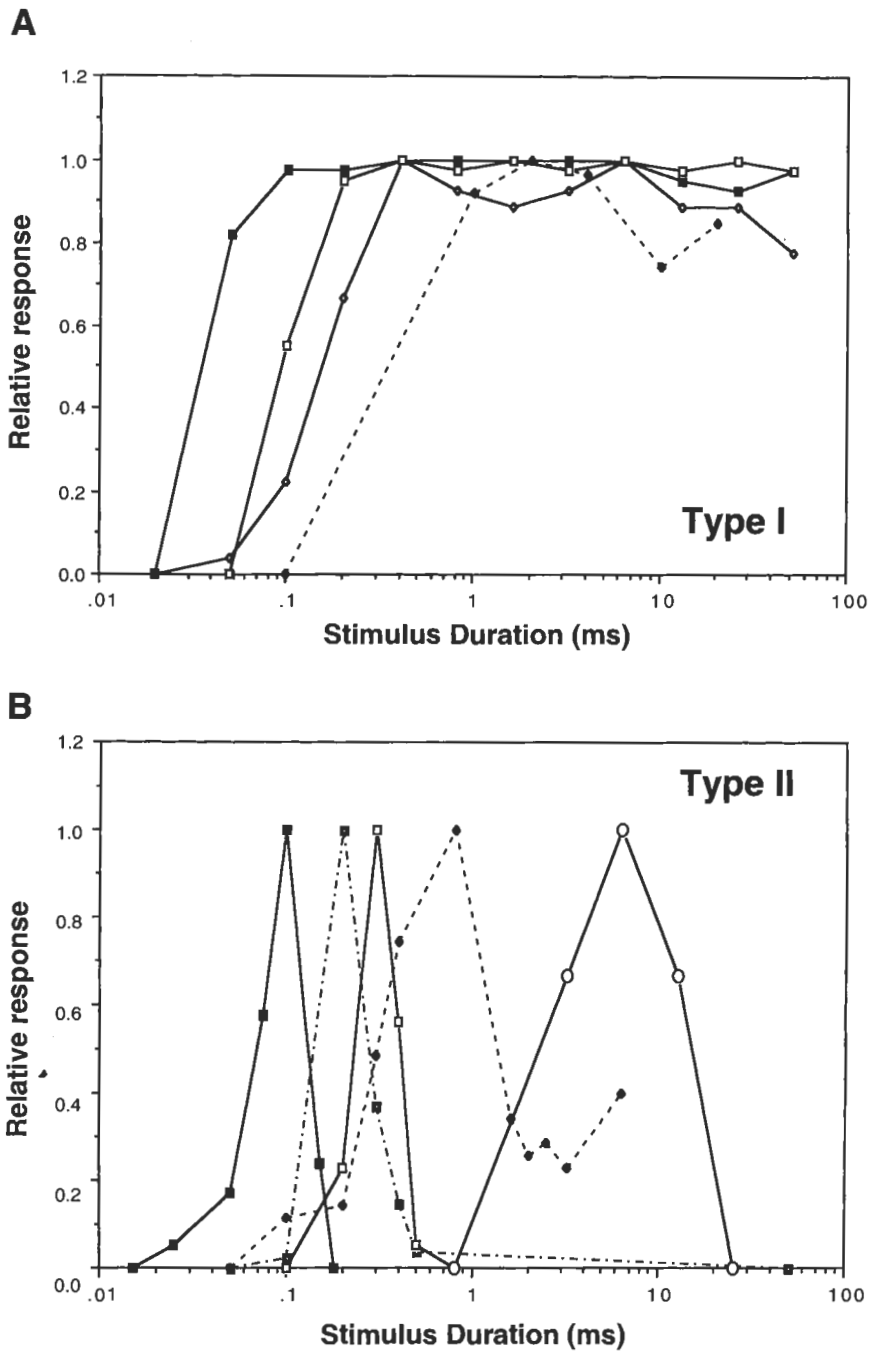

Fig. 4A, B Responses of type I and type II cells. **A** Type I cells. The responses of the cells that are not tuned to specific durations of square-pulse stimuli are plotted as normalized response probabilities. The normalized duration tuning curves show that these cells started to respond to stimuli longer than a certain duration and quickly reached maximum firing rates that were maintained for stimulus durations exceeding 20 ms. **B** Type II cells. Plotted as above, each cell is maximally responsive to a different duration of square wave stimulus

Table 1 Summary of type I and type II cells

Cell type	Response probability	Latency	Time locking	Polarity sensitivity	Amplitude sensitivity
Type I	High	7–9 ms	Strong	Low	Moderate
Type II	Low	12–20 ms	weak	High	High

type I cells were more likely to fire in response to one stimulus polarity than the other, but most type II cells fired only in response to one polarity tested against a combination of intensities (0.1 mV cm^{-1} to 270 mV cm^{-1}) and durations (0.01 ms to 100 ms; Fig. 6A, B; Mann-Whitney U-test, $U_{9,9} = 66$, $P < 0.05$). The polarity of stimulation would alter only the sequence in which different areas of the body were stimulated, for example, in transverse geometry, left-right or right-left portions of the body were stimulated in sequence. Thus, the type II cells responses depended heavily on the sequence of stimulation.

Pharmacological blockade of GABAergic inhibition

According to Mugnaini and Maler (1987), the small cells in ELa are completely covered with GABAergic synapses

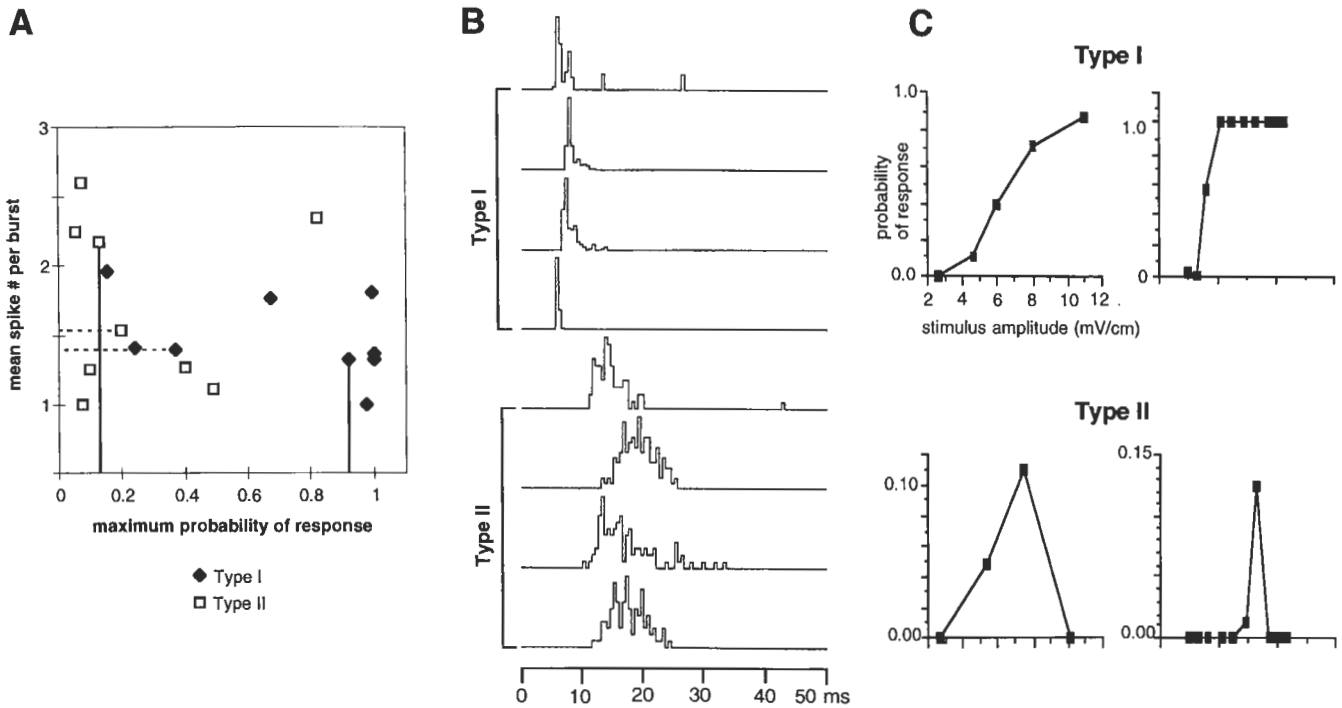

Fig. 5A–C Comparisons of type I and type II cells. **A** The scatter plot shows nine type I cells and nine type II cells according to their individual maximum response probability (*x*-axis; how likely a cell is to fire any spikes when stimulated) and their mean number of spikes per burst (*y*-axis). $r = -0.435$ (Type I; NS $df = 7$), 0.0298 (Type II; NS $df = 7$), –0.263 (all; NS $df = 16$). The two variables are thus unrelated. The *drop bars* to each axis represent median values for type I and type II cells in each variable dimension. The response probability (*x*-axis values) of type I cells is significantly greater than type II cells ($U_{9,9} = 70$, $P < 0.01$; Mann-Whitney U-test). For the average number of spikes per burst (*y*-axis values), there is no statistical difference ($P > 0.05$; *t*-test) **B** Latency. Post-stimulus time histograms for four type I (upper four histograms) and four type II (lower four histograms) cells. Histogram bin width: 500 μs. 200 stimulations in each histogram. **C** Sensitivity of response to stimulus intensity. Responses of type I (*top row*) and type II (*bottom row*) cells are plotted as the probability of response against stimulus intensity. All other stimulus parameters were adjusted at the time of data collection to yield maximal responses. Type II cells are suppressed at high stimulus intensities. Type I cells are typically not suppressed at high stimulus intensities

from the large interstitial cells. To test whether GABA is inhibitory on the small cells, I blocked the GABAergic inhibition with PTX. This was examined using both evoked potential recordings and single cell recordings. After establishing the baseline activity, a 200 $\mu mol \cdot l^{-1}$ solution of PTX in saline was drip-fed into the cranial cavity. After 30 min PTX was replaced with saline for wash-out. The magnitude of the evoked potential rose dramatically within 10 min after the introduction of PTX (Fig. 7A) and the effect was reversible, disappearing after 55 min of wash-out. The largest evoked potential that developed as a result of the PTX treatment had a latency of 6–8 ms which was similar to that of type I cells, but there were also increases in longer latency potentials at 10–15 ms which corresponded to the typical latencies of type II cells. An even longer latency event between 17 ms and 30 ms was also unmasked (Fig. 7A). An example of this effect at the single cell level is seen in Fig. 7B. Initially, this type I cell had a low firing probability with responses consisting of one or two spikes. After PTX, the firing probability increased to 100%, and the responses were bursts of four to seven action potentials. The increased bursting was not accompanied by an increase in the spontaneous discharge rate. These results are consistent with the hypothetical role of GABA as a major inhibitory neurotransmitter in ELa, but PTX may have alternative sites of action, such as yet undiscovered inhibitory neurons within the ELp itself.

Intracellular recording

As described above, the cells of ELp often show very stringent preferences for stimulus parameters while being very susceptible to suppression of response from rapid presentation of stimuli. Because of this selectivity, and because of the difficulty of holding intracellular penetrations of small cells in ELp, characterization of these cells is difficult. In one case the action potential size was sufficiently large (60 mV) to indicate that the recording was truly intracellular. This cell is an example of a type II cell that showed a duration preference to 0.3–0.4 ms (Fig. 8A). The recordings show that action potentials rode on top of an excitatory postsynaptic potential (EPSP) that increased in size for the cell's preferred stimulus duration (Fig. 8A, C). The variability in the amplitude of the EPSP was high, showing overlaps for favorable and unfavorable stimulus durations. When the traces were averaged, three distinct EPSP initial trajectories were seen (Fig. 8B). The relative size of the EPSPs for different stimulus durations roughly paralleled the cell excitability (Fig. 8C).

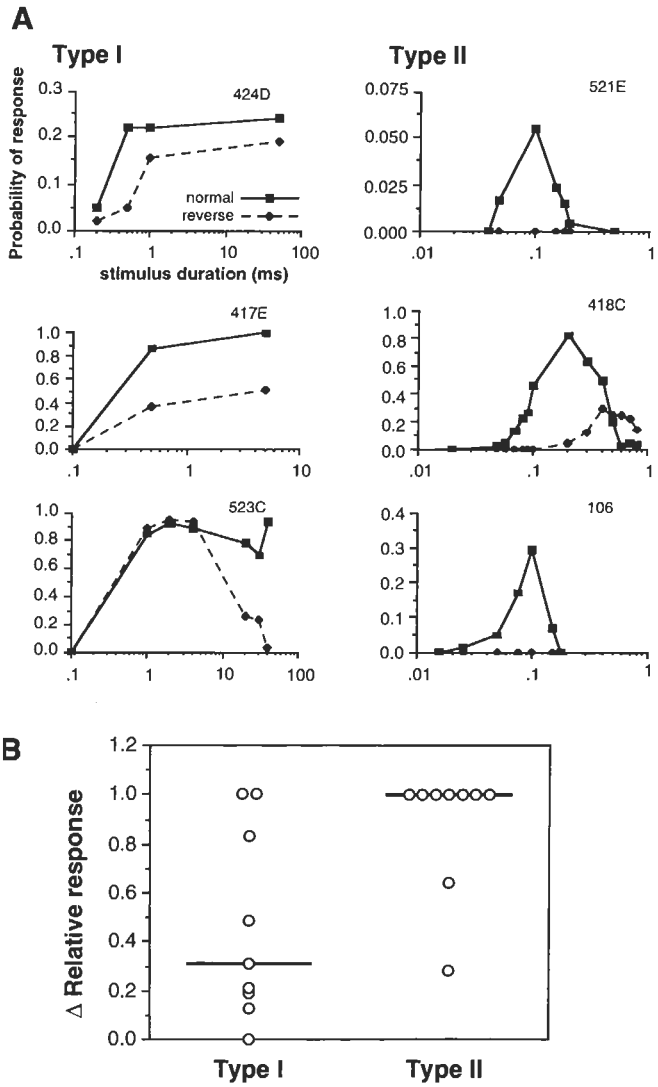

Fig. 6A, B Stimulus polarity sensitivities of type I and type II cells. **A** The probability of response plotted as a function of stimulus duration in two stimulus polarities. The *solid line* is the response to the favored polarity (which might be left followed by right or right followed by left depending on each cell), the *dotted line* to the unfavored polarity. Stimulus amplitude was adjusted for each cell to elicit the best response prior to the collection of final data. *Left column*: type I cells. *Right column*: type II cells. Type II cells were more sensitive to changes in polarity, often showing complete suppression of responses in one polarity. Type I cells were less sensitive, although some cells showed a severe response reduction in one polarity (e.g., unit 417E). Unit 523C illustrates the complex nature of these cells: this cell showed a type I-like duration independence in one polarity, a type II cell-like duration tuning in the other. **B** The polarity sensitivity is measured here as ΔRelative response, defined as the difference in maximum firing probability for the two polarities divided by the maximum firing probability of the cell. If this measure is 1, the cell was completely insensitive in one polarity, if 0, then there was no difference. The graph shows ΔRelative response values for type I and type II cells with the median value shown by a *horizontal bar*. Despite some overlap, type II cells were more sensitive to the polarity of the stimulus ($n = 9$ in each group, $U_{9,9} = 66$, $P < 0.05$; Mann-Whitney U-test)

Discussion

Differences in ELa activity and ELp activity

This is the first report on the physiology of single neurons in ELp of the mormyrid Knollenorgan system. Cells encountered in ELp differed from units in ELa in the following ways. First, while ELa cells were often spontaneously active (Amagai et al. 1998), ELp cells were silent unless stimulated (26 cases out of 29). Second, while an ELa cell responded to nearly any single outside-positive-going voltage step, the response of many ELp cells depended acutely on the stimulus amplitude, geometry and polarity (Figs. 5D, 6A). This was particularly true of type II cells. The dependence was so specific that it was quite possible to miss a cell near the electrode if the search stimulus was unfavorable to that cell. A rapid stimulus presentation rate of more than two to four per second substantially depressed the responsiveness of these cells, limiting the number of cells that could be sampled per preparation. Even with the most favorable stimulus configuration within the experimental setup, most (27 out of 29) ELp cells did not respond to each and every stimulus and typically responded at a much lower rate (Fig. 3C, and other references to response probabilities). Third, when an ELa cell responded to a stimulus, it fired a fixed number of action potentials characteristic of that cell, but when an ELp cell responded, identical stimuli could elicit different latency and number of spikes. Bursting was not uncommon among ELp cells, but a burst does not appear to indicate a particularly favorable stimulus. Finally, ELa cells had a response latency of about 3 ms with very accurate time locking (on the order of 100 μs jitter) when driven strongly (Amagai et al. 1998). ELp cells had a response latency of 6–20 ms with concomitant decrease in the degree of time locking.

The stimulus intensity required to bring either type of cell to maximum firing rate (often more than 10 mV cm^{-1}) was higher than the minimum threshold reported in an earlier study for the Knollenorgan electroreceptors (0.2–1 mV cm^{-1}; Bennett 1965). However, Bennett's measurement was at the receptor openings, while in the present study, the stimulus intensity was that of the stimulus field strength measured along the current path in the experimental tank. Some electroreceptors may not be stimulated by a given stimulus geometry (Yager and Hopkins 1993). The disparity in threshold values between this study and Bennett (1965) can be explained by the differences between the ambient stimulus field strength and the actual stimulus intensity through the pore of the electroreceptor, which varies over the body surface.

Knollenorgan-like aspects of ELp activity

Both the evoked potential and the extracellular single cell experiments revealed that, surprisingly, ELp activity

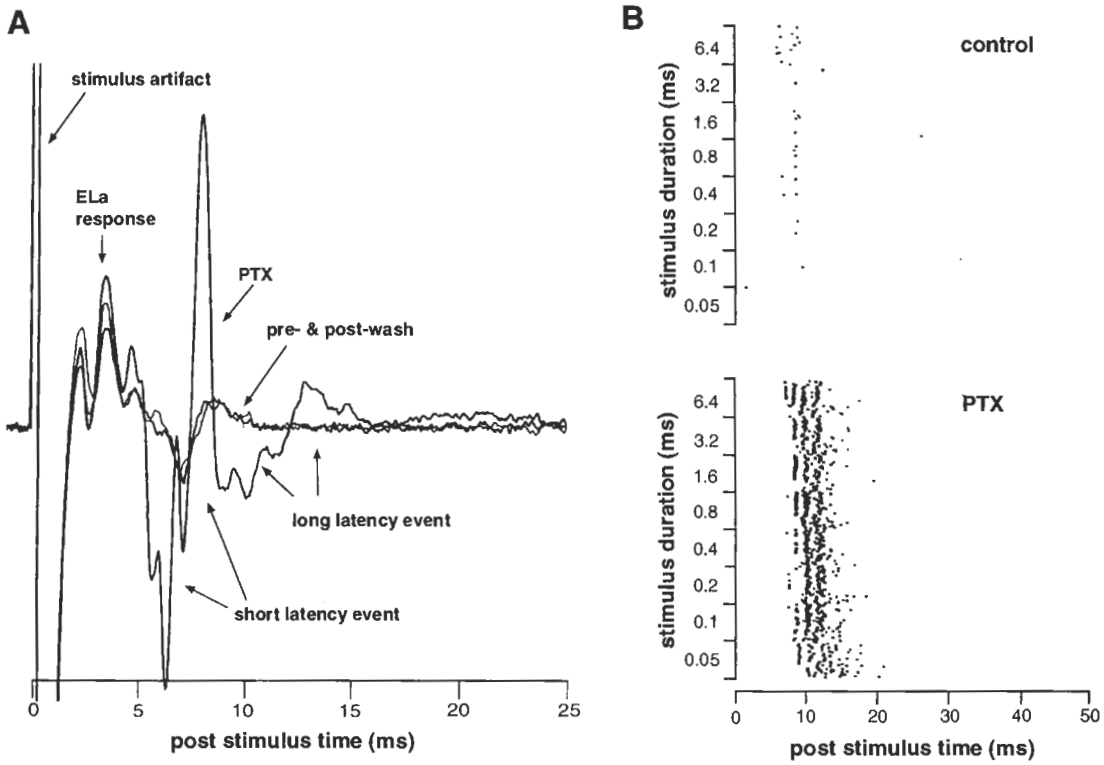

Fig. 7A, B Disinhibition of the cells of ELp. **A** Disinhibition of evoked potential by pharmacological blockade of chloride channels. Three (control, PTX, post-wash) averaged (from five sweeps) evoked potentials recorded in ELp are superimposed. PTX was recorded 25 min after PTX application, post-wash was recorded 50 min after the wash had started. Note that the ELa response recorded by passive spread of current did not change, but later peaks that are in the range of 5–15 ms latency became much larger under treatment by PTX. Short latency events were in the latency range comparable to type I cells, and long latency events in type II cells latency range. An additional slower potential also appears between 17 ms and 35 ms. **B** Disinhibition of a type I cell by PTX. *Top*: raster plots of activity before PTX application. The stimulus is transverse, 6.4 mV cm^{-1} delivered at 2 pps. The raster is subdivided into 40 sweep subrasters of 8 different durations ranging from 0.05 ms to 6.4 ms in a logarithmic scale, separated by tick marks on the *y*-axis. The uppermost subraster was from 6.4 ms, the next below it was from 3.2 ms and so on. A stimulus artifact can be seen next to the *y*-axis for stimulus durations of 0.1 ms or more. The cell responded to a stimulus of almost any duration with a single spike of 7–10 ms in duration. At longer duration of stimuli, the responses were slightly greater. *Bottom*: 10 min after application of 0.3 mmol·l^{-1} PTX in the cranial cavity. The stimulus regime was otherwise identical. Under this condition, the type I cell was disinhibited, firing many bursts of multiple action potentials, even down to 0.05 ms stimulus duration

shares many characteristics with that of the Knollenorgan receptors, even though ELp is thought to be situated downstream from the site of critical temporal analysis of EODs. In particular, type I cells, which have response latencies that match those of the evoked potentials observed in ELp, respond to simple voltage steps just as Knollenorgans do. The minimum stimulus duration threshold of at least some type I cells also matches that of Knollenorgans (C. C. Bell, personal communication), although others had much longer minimum durations. The relative sizes of field potentials that correspond to stimulations of different parts of the body are in accordance with the known projections of the Knollenorgan pathway; one-third of all Knollenorgans are located in the head region while the other two-thirds are distributed evenly between the dorsal and ventral areas, with a slight bias towards the head (Harder 1968). Also, while the projection from NELL to ELa is bilateral, the contralateral projection is heavier than ipsilateral projection (Szabo et al. 1983), consistent with the larger field potential that is elicited by the stimulation of the contralateral body surface. Furthermore, the regional distribution of ELp-evoked potentials shows that the stronger potentials were recorded closer to the border with ELa and weaker potentials were recorded in the peripheral areas of ELp. The spatial distribution of evoked potentials in ELp parallels the projection pattern of the fiber tracts between ELa and ELp. The output fibers of ELa are concentrated in the center of the roughly circular border between the two nuclei and then fan out to cover the various parts of ELp (Friedman 1995, 1997). The structure of ELp is nuclear and not organized in discrete laminae. The cells responsible for analysis of temporal information may be distributed diffusely throughout the nucleus rather than concentrated in a distinct layer. If only a subset of the neurons are sensitive to temporal cues, their activities could be masked by the more prevalent information throughput from ELa, which could explain the apparent lack of temporally sensitive evoked potentials in ELp. Based on these factors, I propose that the gross evoked

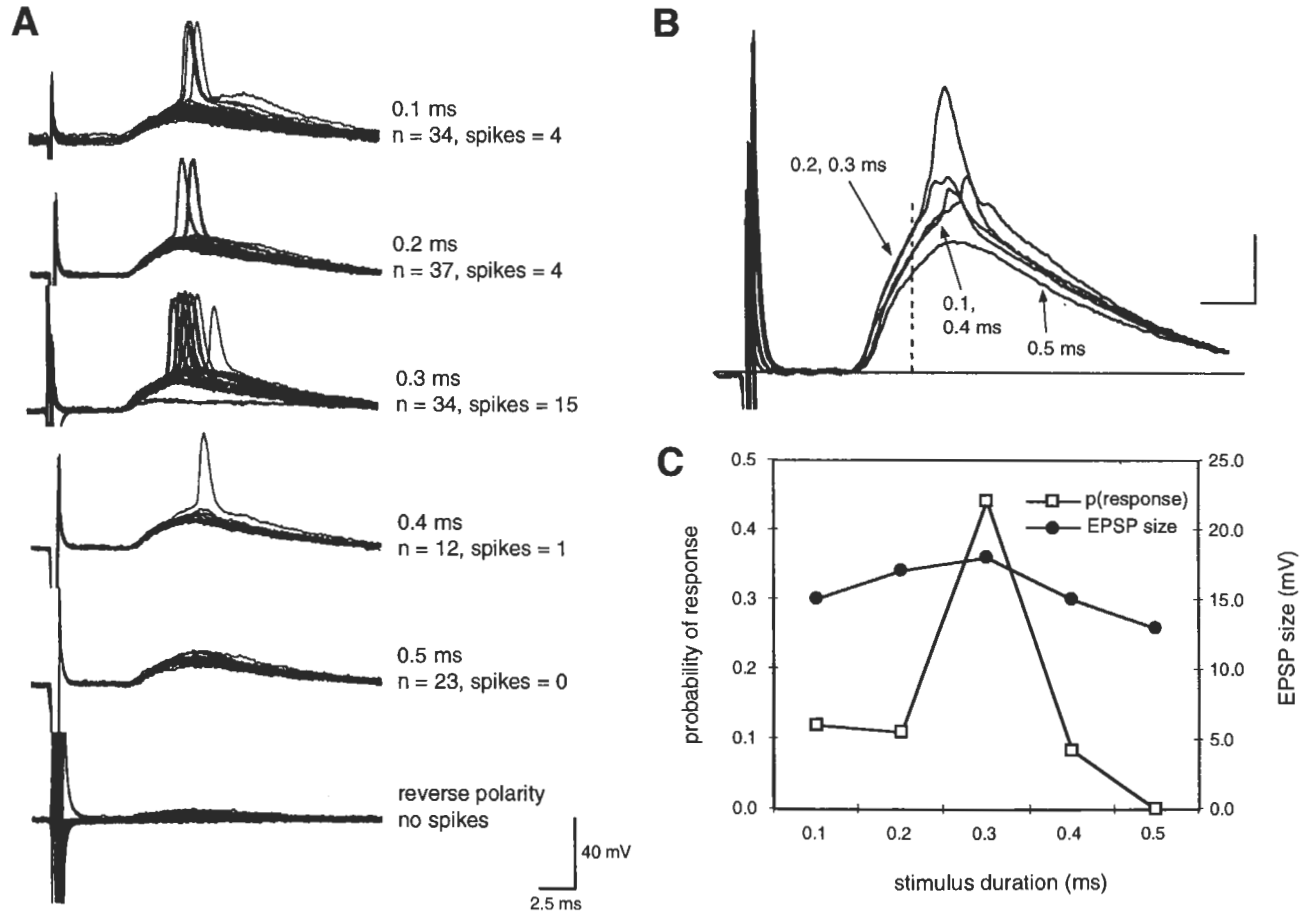

Fig. 8A–C Intracellular recordings of a type II cell. **A** Superimposed traces of type II cell activity in response to variable duration stimuli. The cell was most responsive to a stimulus duration of 0.3 ms. At greater than 0.5 ms, the action potentials were completely abolished, even though some EPSPs remained. If the polarity of the stimulus was reversed (*bottom*; superimposed traces of stimulus durations 0.1 to 1 ms), even these residual EPSPs were attenuated. The onset of the EPSP is 6 ms after the stimulus. The EPSP amplitude varied greatly for the same stimulus duration. **B** Data from each duration in **A** was averaged then superimposed. Unusual-looking spikes occurring at the peak are the result of averaging action potentials occurring at different times. Three distinct levels of EPSPs were detected, the lowest at 0.5 ms, the next lowest at 0.1 and 0.4 ms, the highest at 0.2 and 0.3 ms. To quantify the relative strength of the EPSPs, the amplitude from the resting potential was measured at the arbitrarily chosen *dotted line*. The line was drawn through a time before any of the action potentials began to avoid contamination of the averaged waveforms. **C** EPSP size (*closed circles*) and cell response (*open squares*) as a function of stimulus duration

potentials observed here are made up of summed activity of type I cells.

Cells that are tuned to duration of stimuli (type II cells)

I have also shown that ELp type II neurons are sensitive to temporal features of the stimuli, a property that is not visible in ELa. The peak sensitivities of these neurons span a wide range of stimulus durations (at least two orders of magnitude), sufficiently diverse to encode a variety of waveforms. However, type II neurons are remarkably un-responsive, responding to a stimulus less than one in five times on average, even at the most favorable stimulus parameters. While the type II cells' response probability may indeed be low in free-swimming fish, it is possible that my limited stimulus set did not contain the precise stimulus characteristics to drive the unit effectively. Preliminary experiments using natural EODs as stimuli (not shown) did not appear to appreciably increase type II cell responsiveness, but uses of a wider variety of stimulus characteristics should be pursued further.

Type II cells are also sensitive to a variety of stimulus features including amplitude, polarity and repetition rate. One could therefore argue that the Knollenorgan pathway is not only instrumental in analyzing the temporal features of the stimuli, but also to direction and strength of the electric field generated by other fish. Since the Knollenorgan electroreceptors do not encode amplitude of the stimulus very well (Hopkins 1981), these other possible stimulus parameters have often been neglected when considering the Knollenorgan system. However, Knollenorgans will individually experience different degrees of stimulation depending on the local strength of the electric field, determined by the direction of stimulus current with respect to the body. When the local stimulus intensity is near threshold for a Knollen-

organ, the timing of the action potential generation will vary (Amagai et al. 1998). Exactly when the spike occurs will be determined in a probabilistic manner depending on what portion of the stimulus waveform is outside positive (Arnesen and Hopkins 1985).

Deducing the processing in ELa based on activities in Elp

Mugnaini and Maler (1987) concluded that the small cells of ELa that project to ELp receive electrotonic excitatory inputs from NELL afferents and heavy GABAergic synaptic inputs from the large cells of ELa, presumably for inhibition. Based on their relative response latencies (Fig. 9A), I propose that type I cells represent output cells of ELa or cells that are not too far downstream from ELa small cell output. One possibility is that the small cells of ELa are inhibited for a specific stimulus duration, while firing normally for all other durations. The results shown here do not demonstrate such a depression of activity, indicating either the original model based on Muganini and Maler (1987) and outlined in Amagai et al. (1998) is incorrect or that type I cells are not the same as the small cell axons. On the other hand, in the counter-current model of ELa organization suggested in the companion paper (Amagai et al. 1998) the output cells of ELa are active for stimulus durations above a minimum threshold much like the ELp type I cells shown here. The blockade of chloride channels disinhibits both the evoked field potential and the activity of type I cells, consistent with the hypothesis that they represent output activities of ELa in the model. However, it is also possible that GABA plays a significant role within ELp itself, so the pharmacological effects observed here may be happening entirely within ELp. If ELa small cells act as conventional coincidence detectors as suggested as a possibility in the companion paper (Amagai 1998), then the small cells should increase their activities when the stimulus is at a specific duration. This model is not supported given the prevalence of activity in ELp to a simple voltage step and not tuned to a stimulus duration.

The model of temporal analysis in ELp

The latency of the EPSPs seen in a type II cell (onset at 6 ms; Fig. 8A) does fall within the range of type I cell

Fig. 9A, B Model of temporal analysis in ELp. **A** Latencies of three cell types in ELa/p. PSTHs of the NELL axons to ELa, type I cell of ELp and type II cell of ELp are shown. Bin size: 500 μs. **B** Two type I cells selected from the data set are plotted at top. *y*-axis: normalized response, *x*-axis: stimulus duration. type I cell (*A*) has a minimum stimulus duration that is lower than that of type I cell (*B*). Thus, if they counteract, i.e., *A* is excitatory while *B* is inhibitory, then there is a window of excitability that can be extracted by a hypothetical postsynaptic cell shown below. (The response plotted is A–B.) The resulting duration selectivity mimics that of a type II cell

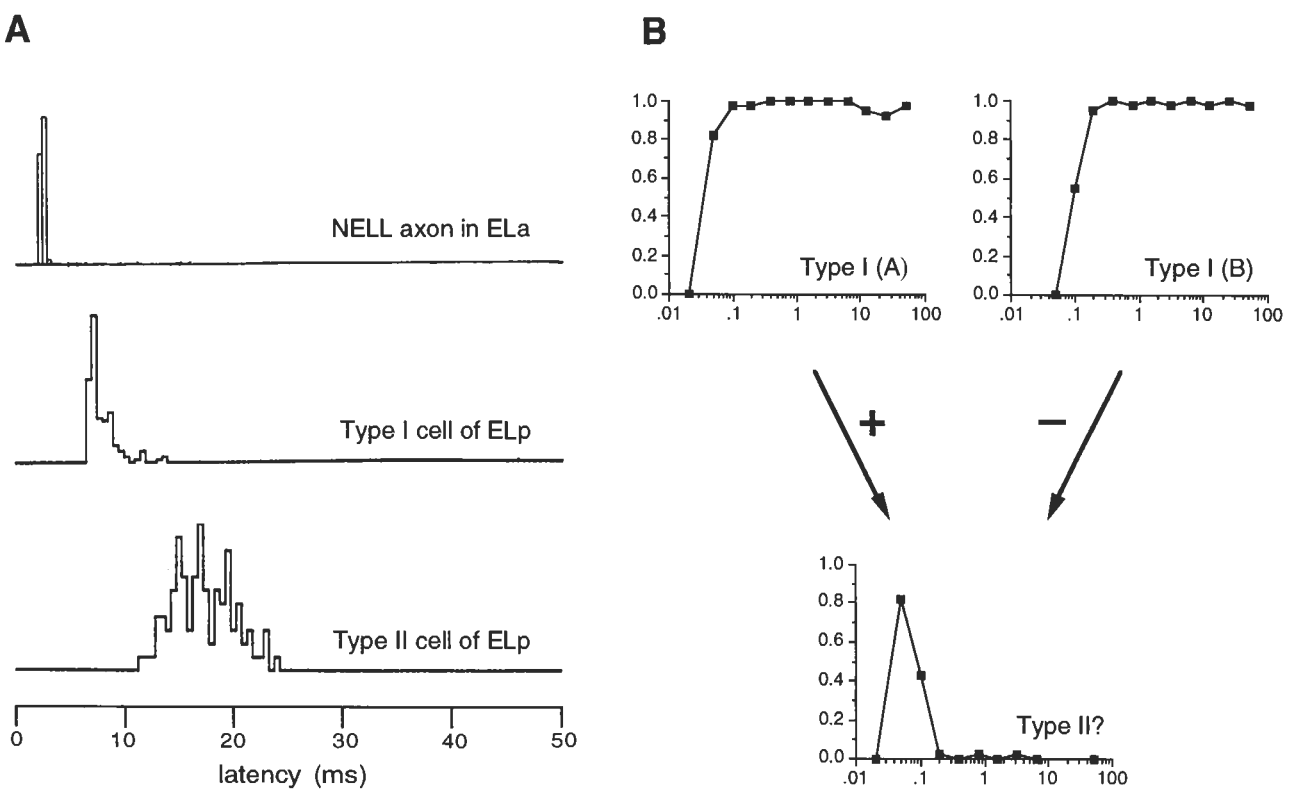

latencies (6–10 ms; Fig. 5B). Type II cell firing latencies are consistently longer than type I cell latencies (Fig. 5B). Therefore, type II cells could be postsynaptic to type I cells. The simplest way to create a type II cell response pattern from type I cells would be to have two type I cells with different duration thresholds converge on a single type II cell, as represented in Fig. 9B. Here, two type I cells, one excitatory, the other inhibitory, converge on a single cell. Because the minimum duration for type I cell (A) is lower than that of (B), the window of excitability resembles that of a type II cell, with a peak around 0.5 ms. Polarity sensitivity that is common in type II cells could be generated if type I cell A or B has a reduced response to one polarity of stimulus, causing the summed activity to be subthreshold for all durations in one polarity but not the other. An important feature of this model is the minimum duration sensitivities of type I cells, which could arise out of the countercurrent information flow and the collision of excitatory and inhibitory inputs in ELa described in (Amagai et al. 1998).

I emphasize that timing of the action potential in type I cells need not be precise, as long as they are able to overlap closely enough in time in the postsynaptic neuron. This type of information re-coding from representation by timing to representation by cellular identity could allow the system to maintain the accuracy of temporal representation without the need for neurons with high temporal fidelity. Neural structures that are capable of carrying accurate representations of fine temporal features seem to require many specializations (Carr and Amagai 1996). Presumably, it will be an evolutionary advantage to minimize the extent of nervous tissue specialized to such an extent.

Even though this model is the simplest explanation for my observations, details of the characteristics of type I cells remain unexplained. For example, the activity of some type I cells showed complex dependence on stimulus polarity or amplitude. Further, categories designated as type I cells may actually be a heterogeneous mixture of several ELp cell types as well as the ELa output cells. The classification of ELp cells into types I and II, though empirically defined purely on the basis of whether a single voltage step can excite the cell, is largely to facilitate description. It will require further work to establish if they are anatomically uniform classes of cells. Also, both types I and II cells show tendencies to fire in bursts, but what governs the number of action potentials per burst is unknown, especially since there is no correlation between a cell's responsiveness and its tendency to burst (Fig. 5A).

In addition to the inputs from ELa, ELp also receives inputs from at least three other nuclei, including the nucleus isthmi, ventral anterior medial nucleus of the torus longitudinalis and an unnamed perilemniscal group of cells, while sending outputs to the nucleus isthmi, inferior olive, nucleus medialis ventralis and the sub-praeminential nucleus (Haugedé-Carré 1979; Bell et al. 1981; Finger et al. 1981). Clearly this is a nucleus that is a major nexus of information.

Acknowledgements This work was supported in part by an NIMH grant MH37972 to Carl Hopkins and Rosenblatt Fellowships. I thank Jud Crawford, Philip Stoddard, Jessica McKibben and Carl Hopkins for helpful comments and discussion, Matthew Friedman for indispensable help with discussion and manuscript preparation, Garry Harned for help at many stages of the research and an anonymous reviewer for many helpful comments.

References

Amagai S, Friedman MA, Hopkins CD (1998) Time coding in the midbrain of mormyrid electric fish I: physiology and anatomy of cells in the nucleus exterolateralis pars anterior (ELa). J Comp Physiol A 182: 115–130

Arnesen SJ, Hopkins CD (1985) Electroreceptor tuning predicts temporal encoding of species-specific signals in electric fish. Soc Neurosci Abstr 11: 270

Bell CC (1986) Electroreception in mormyrid fish: central physiology. In: Bullock TH, Heiligenberg W (eds) Electroreception. Wiley, New York, pp 423–452

Bell CC, Szabo T (1986) Electroreception in mormyrid fish: central anatomy. In: Bullock TH, Heiligenberg W (eds) Electroreception. Wiley, New York, pp 375–421

Bell CC, Finger TE, Russell CJ (1981) Central connections of the posterior lateral line lobe in mormyrid fish. Exp Brain Res 42: 9–22

Bennett MVL (1965) Electroreceptors in mormyrids. Cold Spring Harbor Symp Quant Biol 30: 245–262

Bennett MVL, Steinbach AB (1969) Influence of electric organ control system on electrosensory afferent pathways in mormyrids. In: Llinas R (ed) Neurobiology of cerebellar evolution and development. American Medical Association, Chicago, pp 207–214

Carr CE, Amagai S (1996) Processing of temporal information in the brain. In: Pastor MA, Artieda J (eds) Time, internal clocks and movement. Elsevier, Amsterdam, pp 27–52

Dowben RM, Rose JE (1953) A metal-filled microelectrode. Science 118: 22–24

Enger PS, Libouban S, Szabo T (1976) Rhombencephalic connections in the fast conducting electrosensory system of the mormyrid fish, *Gnathonemus petersii*. An HRP study. Neurosci Lett 3: 239–243

Finger TE, Bell CC, Russell CJ (1981) Electrosensory pathways to the valvula cerebelli in mormyrid fish. Exp Brain Res 42: 23–33

Friedman MA (1995) The projection within the nucleus exterolateralis in the knollenorgan pathway of mormyrid fish. Soc Neurosci Abstr 21: 187

Friedman MA (1997)) Mechanisms of temporal analysis in the knollenorgan electrosensory system of mormyrid fish. PhD thesis, Cornell University, Ithaca, New York

Graff C, Kramer B (1992) Trained weakly-electric fishes *Pollimyrus isidori* and *Gnathonemus petersii* (Mormyridae, Teleostei) discriminate between waveforms of electric pulse discharges. Ethology 90: 279–292

Harder (1968) Die Beziehungen zwischen Elektrorezeptoren, elektrischem Organ, Seitenlinienorganen und Nervensystem bei den Mormyridae, Teleostei, Pisces. Z Vergl Physiol 59: 272–318

Haugedé-Carré (1979) The mesencephalic exterolateral posterior nucleus of the mormyrid fish *Brienomyrus niger*: efferent connections studied by the HRP method. Brain Res 178: 179–184

Haugedé-Carré (1980) Contribution a l'étude des connexions du torus semicircularis et du cervelet chez certains mormyrides. Ph.D. thesis, L'Université Pierre et Marie Curie, Paris

Hopkins CD (1981) Functions and mechanisms in electroreception. In: Northcutt JP, Davis RE (eds) Fish neurobiology. University of Michigan Press, Ann Arbor, pp 215–259

Hopkins CD (1986) Behavior of Mormyridae. In: Bullock TH, Heiligenberg W (eds) Electroreception. Wiley, New York, pp 527–576

Hopkins CD, Bass AH (1981) Temporal coding of species recognition signals in an electric fish. Science 212: 85–87

Hopkins CD, Westby GWM (1986) Time-domain processing of electric organ discharges by pulse-type electric fish. Brain Behav Evol 29: 77–104

McGregor PK, Westby GWM (1992) Discrimination of individually characteristic electric organ discharges by a weakly electric fish. Anim Behav 43: 977–986

Moller P, Szabo T (1981) Lesions in the nucleus mesencephali exterolateralis: effects on electrocommunication in the mormyrid fish *Gnathonemus petersii* (Mormyriformes). J Comp Physiol 144: 327–333

Mugnaini E, Maler L (1987) Cytology and immunocytochemistry of the nucleus extrolateralis anterior of the mormyrid brain: possible role of GABAergic synapses in temporal analysis. Anat Embryol 176: 313–336

Russell CJ, Bell CC (1978) Neuronal responses to electrosensory input in the mormyrid valvula cerebelli. J Neurophysiol 141: 1495–1510

Szabo T, Enger PS, Libouban S (1979) Electrosensory systems in the mormyrid fish, *Gnathonemus petersii*: special emphasis on the fast conducting pathway. J Physiol (Paris) 75: 409–420

Szabo T, Ravaille S, Libouban S, Enger PS (1983) The mormyrid rhombencephalon: I. Light and EM investigations on the structure and connections of the lateral line lobe nucleus with HRP labelling. Brain Res 266: 1–19

Yager DD, Hopkins CD (1993) Directional characteristics of tuberous electroreceptors in the weakly electric fish, *Hypoponnus* (Gymnotiformes). J Comp Physiol A 173: 401–414